Optimization of the Magnetic Sensor Configuration for JT-60SA Plasma Control*)

Manabu TAKECHI, Mitsuhiro SUZUKI, Yoshiaki MIYATA, Kenichi KURIHARA, Takahiro SUZUKI and Shunsuke IDE

National Institutes for Quantum and Radiological Science and Technology, Naka, Ibaraki 311-0193, Japan

(Received 6 January 2018 / Accepted 9 March 2018)

The number of magnetic probes and flux loops required for a sufficiently accurate plasma surface reconstruction of JT-60SA are investigated by applying the Cauchy condition surface (CCS) method. For this purpose, CCS reconstruction parameters, CCS size and the number of CCS nodes, were optimized using the various combinations of limited number of magnetic sensors. The highly accurate reconstruction within the 1 cm divertor-hit-point error in the JT-60SA plasma can be obtained by optimizing the CCS reconstruction parameters. Once the minimum sensor configuration is found, we can optimize the number of sensors and the related data acquisition systems.

Keywords: plasma surface reconstruction, magnetic sensor, Cauchy condition surface, last closed flux surface

DOI: 10.1585/pfr.13.3402118

1. Introduction

The measurement of the plasma shape and position plays the most basic and important role for both plasma operation and its assessment. For example, the ellipticity and triangularity of the plasma poloidal cross section affecting transport and magneto hydro dynamics (MHD) stability can be considered for assessment. The clearance between the plasma surface and the conductive wall changes the resistive wall mode (RWM) stability. In addition, we need to control the divertor strike points for safe plasma operation.

JT-60SA, which has completely superconducting coils, has been designed and recently constructed for the supplementing ITER toward DEMO [1], after approximately 18 years of JT-60U's operation. To obtain information regarding JT-60SA plasma control and physics, many types of magnetic sensors have been developed [2]. For JT-60SA, the reconstruction of plasma's last closed flux surface (LCFS) will be performed with magnetic sensors using the Cauchy condition surface (CCS) method as an inverse problem in real time [3]. The CCS method employs magnetic field signals obtained from magnetic probes (MPs) and magnetic flux signals from flux loops (FLs) for the Dirichlet and Neumann conditions, respectively, in addition to a poloidal coil current.

Generally, the number of the sensors required for plasma equilibrium reconstruction is determined based on the results of using previous or current experimental devices with redundancy for the failure of the sensors. It is well known that an increase in the number of sensors deceases the reconstruction error [4]. However, the cost of magnetic sensors used for plasma control and for their data acquisition systems in large devices possessing a long discharge is high. Therefore, it is considerably important to know the minimum number of the magnetic sensors required for accurately performing plasma surface reconstruction. Herein, we investigated the minimum required number of the MPs and FLs of JT-60SA using the CCS method.

2. Reconstruction of the Plasma Surface Using the CCS Method

Using the CCS method, the LCFS is reconstructed with a magnetic sensor signal and poloidal coil current. Both Dirichlet [magnetic field (B_θ)] and Neumann [flux (ϕ)] conditions at the CCS nodes in the plasma were calculated based on the magnetic sensor signals [3]. Figure 1 shows a typical poloidal cross section of the JT-60SA plasma, CCS, CCS nodes, and magnetic sensors. The flux distribution outside the CCS is calculated from B_θ and ϕ. The LCFS is determined by the points at which ϕ is same as that at X or the limiter point. It should be noted that no information inside the plasma, such as current and pressure profile, is required. The validity of the CCS method was verified via actual experiments [5].

Real-time calculations with CCS method were performed in JT-60U for plasma control and analysis. Moreover, the plasma current and its distribution can be evaluated using the CCS method [4]. The preliminarily unknown eddy current distribution in the vacuum vessel is reconstructed in a reversed field pinch device based on the external magnetic sensor signals [6]. Furthermore,

author's e-mail: takechi.manabu@qst.go.jp

*) This article is based on the presentation at the 26th International Toki Conference (ITC26).

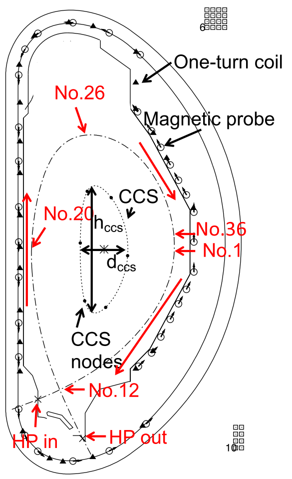

Fig. 1 Typical poloidal cross section of the JT-60SA plasma, Cauchy condition surface (CCS), CCS nodes, and magnetic sensors. The reconstruction error is measured at the last closed flux surface (LCFS) from No. 1 to No. 36 and hit points (HPs) out and in.

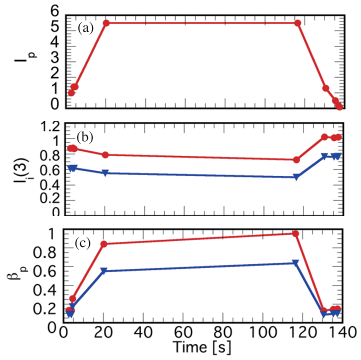

Fig. 2 Temporal evolution of (a) the plasma current I_p, (b) the internal inductance $l_i(3)$, and (c) the poloidal beta β_p of JT-60SA for the optimization of the CCS parameters.

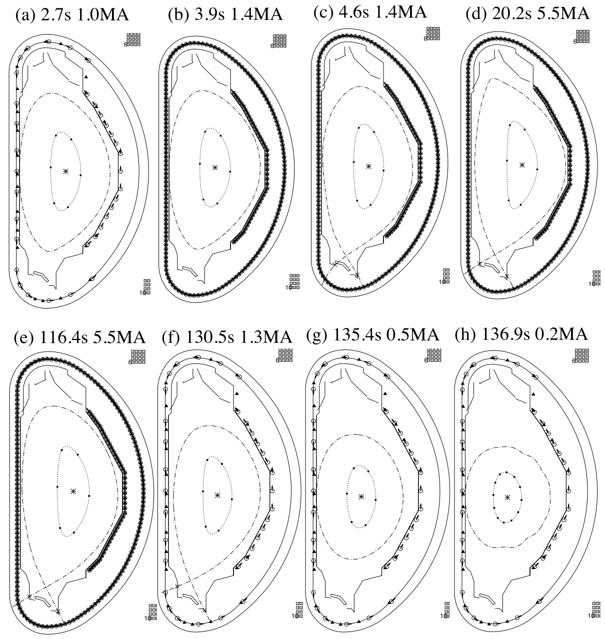

Fig. 3 Snap shots of the poloidal cross-section of the JT-60SA plasma for CCS evaluation.

the CCS method has been expanded to reconstruct the 3D magnetic field profile outside the non-axisymmetric plasma in the Large Helical Device (LHD) [7].

3. Optimization of CCS Reconstruction Parameters

We optimized the CCS reconstruction parameters with JT-60SA plasmas before we identified the minimum number of sensors. The CCS reconstruction parameters include the CCS size, number of CCS nodes, and weight for the weighted least squares method. The size and position of the CCS do not influence the accuracy of the CCS reconstruction, if multiple sensors exist. However, we must consider these conditions for using the CCS method with a limited number of sensors. Considering previous work on this topic, the numbur of CCS nodes applied to JT-60U plasmas was $M = 6$. However, the optimum number of the CCS nodes is supposed to depends on CCS size and the number of sensors. In addition, the effect of the sensor noise was considered.

The parameters were tuned to reduce the reconstruction error at the divertor hit points (HPs) within 1 cm and avoid the LCFS contacting the first wall. The full current JT-60SA plasma with $I_p = 5.5$ MA, $\beta_p = 0.55$ and 0.83, and $l_i(3) = 0.79$ and 0.55 was employed for optimization. Figure 2 shows the temporal evolution of the plasma's parameters. We found that the error was large due to low l_i and that β_p had a slight impact on the error. Therefore, herein, we present the reconstruction results for the plasma with low $l_i(3) = 0.55$. The evaluation of CCS reconstruction was performed at 8 snapshots (Fig. 3) as follows:

(a.) 2.7 s, 1.0 MA, Limiter
(b.) 3.9 s, 1.4 MA, Limiter
(c.) 4.6 s, 1.4 MA, Diverter
(d.) 20.2 s, 5.5 MA, Start of Flat top (SOF)
(e.) 116.4 s, 5.5 MA, End of Flat top (EOF)
(f.) 130.5 s, 1.3 MA, Diverter
(g.) 135.4 s, 0.5 MA, Limiter
(h.) 139.6 s, 0.2 MA, Limiter

The reference equilibria were produced with the TOSCA equilibrium code. The plasma boundary was reconstructed using CCS with B_θ, ϕ and the poloidal coil currents from the TOSCA calculation results. The reconstruction error at the LCFS is defined as the difference between the CCS and reference equilibria, which is expressed as follows:

$$Error\ [m] = \frac{\psi_{\mathrm{surf(ref)}} - \psi_{\mathrm{surf(CCS)}}}{|\psi_{\mathrm{surf(ref)}}|}, \qquad (1)$$

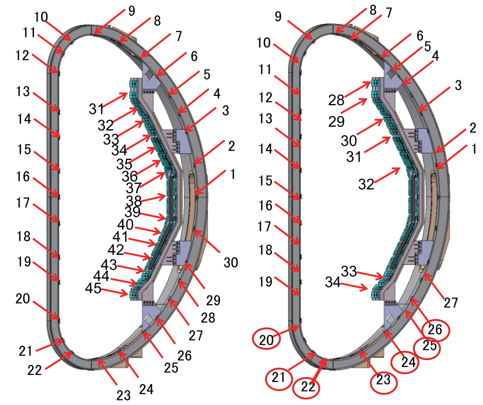

Fig. 4 Realistic maximum number and position of magnetic sensors in JT-60SA. Circled numbers show weighted flux loop.

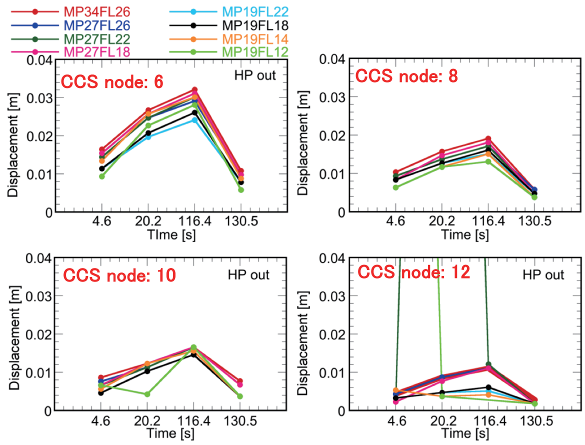

Fig. 5 Reconstruction error of HP out at four times with various number of CCS nodes.

whereas the error at the divertor hit point is defined as distance between the CCS and the reference points. The CCS center was set at the center of the plasma current. Initially, the CCS size was determined based on the CCS hight (h_{CCS}) and CCS width (d_{CCS}), which are half of the plasma height and one-third of the plasma width, respectively. For JT-60U, h_{CCS} and d_{CCS} were 1.2 and 0.8 m, respectively. The triangularity of the CCS was same as that of the plasma. However for JT-60U, triangularity was not used. Initially, 6 CCS nodes were used.

Figure 4 shows the realistic maximum number and position of the magnetic sensors. Herein, the sensors on the VV behind the stabilizing plate (SP) were not used because these signals were shielded by the SP. Therefore, the maximum number of MPs and FLs was 34 and 26, respectively. CCS reconstruction was performed with 9 sensor combinations of 17-34 MPs and 12-26 FLs.

The effect of the magnetic sensor noise on CCS reconstruction error was investigated. To increase the signal-to-noise ratio, we adopted the magnetic sensors with the large coupling area that were same as those adopted for JT-60U [2]. The maximum noise of the MPs and FLs was estimated to be approximately 1 Gauss and 0.0005 Wb based on the experimental results for JT-60U. In addition, 100 different CCS reconstruction were performed with a random noise applied to each sensor signal. As the number of sensors decreased, the error caused due to noise increased. However, the maximum error was within 2 mm even in the case of the smallest number of this assessment. Furthermore, we decided that the effect of the noise can be ignored.

Next, we investigated the effect of CCS nodes on this reconstruction. As the number of CCS node increased, HP errors decreased as shown in Fig. 5. In the case of 12 CCS nodes, the error was reduced to almost within 1cm. However, as shown in Fig. 6, as the number of CCS node increased, the calculation failure or false results (where the LCFS exists inside the CCS) increased, particularly with

6 and 8 CCS nodes

	2.7s	3.9s	4.6s	20.2s	116.4s	130.5s	135.4s	136.9s
MP34FL26	○	○	○	○	○	○	○	○
MP27FL26	○	○	○	○	○	○	○	○
MP27FL22	○	○	○	○	○	○	○	○
MP27FL18	○	○	○	○	○	○	○	○
MP19FL22	○	○	○	○	○	○	○	○
MP19FL18	○	○	○	○	○	○	○	○
MP19FL14	○	○	○	○	○	○	○	○
MP19FL12	○	○	○	○	○	○	○	○
MP17FL19	○	○	○	○	○	○	○	○

10 CCS nodes

	2.7s	3.9s	4.6s	20.2s	116.4s	130.5s	135.4s	136.9s
MP34FL26	○	○	○	○	○	○	○	○
MP27FL26	○	○	○	○	○	○	○	○
MP27FL22	○	○	○	○	○	○	○	○
MP27FL18	○	○	○	○	○	○	○	○
MP19FL22	○	○	○	○	○	○	○	△
MP19FL18	○	○	○	○	○	○	○	△
MP19FL14	○	○	○	○	○	○	○	○
MP19FL12	○	△	△	△	○	○	○	△

12 CCS nodes

	2.7s	3.9s	4.6s	20.2s	116.4s	130.5s	135.4s	136.9s
MP34FL26	○	○	○	○	○	○	○	○
MP27FL26	△	○	○	○	○	△	○	○
MP27FL22	○	○	○	△	○	○	○	△
MP27FL18	△	○	○	○	○	○	×	×
MP19FL22	○	○	△	△	△	△	△	×
MP19FL18	○	○	○	△	△	△	△	△
MP19FL14	△	△	△	△	△	△	○	×
MP19FL12	△	×	△	△	×	△	△	×

Fig. 6 Effect of CCS nodes on reconstruction possibility. Circles, triangles and crosses means reconstruction enable, reconstruction failure (LCFS inside CCS) and calculation failure, respectively.

a small number of sensors and/or small plasma current at t = 136.9 s. Therefore, either 8 and 10 CCS nodes are suitable. However, the reconstruction error of HP cannot be < 1 cm.

B_θ and ϕ at the CCS nodes were determined using the least squares method with magnetic sensor signals. To reduce the reconstruction error to 1cm, we tried to weight the flux loop signals (indicated by circled numbers around the HP in Fig. 4).

Figures 7 (a) and 7 (b) show the reconstruction error at

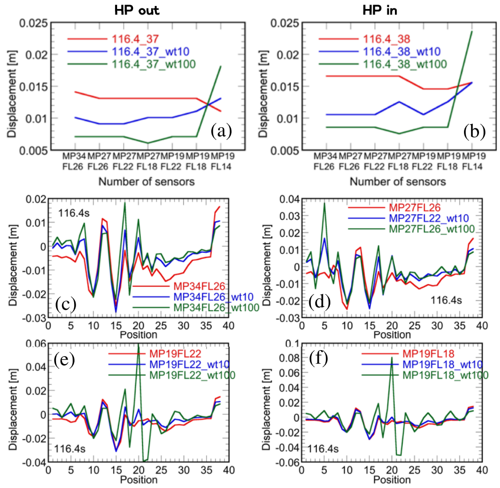

Fig. 7 Reconstruction error at (a) HP in, (b) HP out and (c-f) LCFS without and with weight of 10 and 100 at 116.4 s.

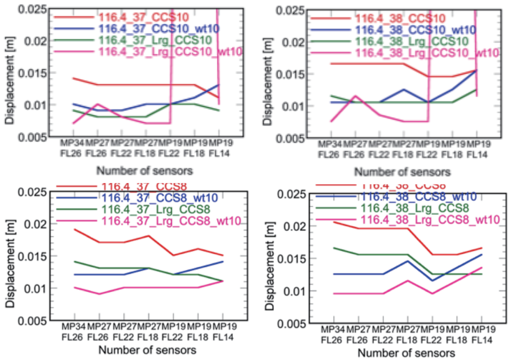

Fig. 8 Reconstruction error at the HP with weights and a large CCS at 116.4 s.

the HPs without and with weights of 10 and 100 at 116.4 s. The error present at the HP is < 1 cm with a weight of 100. However, with a weight of 100, a considerably large error occurs at the LCFS as shown in Figs. 7 (c) - 7 (f) Therefore, herein, 10 as the weight; however, the error cannot be reduced to within 1 cm.

Finally, the effect of the CCS size on the reconstruction error was examined. As $l_i(3)$ decrease, the error increase because the plasma current inside the CCS decreases. Hence, we enlarged the CCS size to reduce the reconstruction error. The height and width of the CCS were increased from half to two-third and from one-third to half of that of the plasma, respectively. The area of the CCS was increased approximately twice. The CCS reconstruction errors were evaluated with a large CCS and with 8 and 10 CCS nodes.

Figure 8 shows the reconstruction error at the HP without and with a weight of 10, a large CCS and 8 and 10 CCS nodes at 116.4 s. The HP error decrease to much less than 1 cm if a large CCS, a weight of 10, and 10 CCS nodes are employed. However, reconstruction failure may occur occationally. The HP error decrease to slightly less than 1 cm if a large CCS, a weight of 10, and 8 CCS nodes are employed. The improvement in the error due to the weight and CCS expansion with 8 CCS nodes was larger than that with 10 nodes. No calculation failure was observed. The reconstruction error at the LCFS between 8 and 10 CCS nodes is compared in Fig. 9. With less number of sensors, the error at the LCSF with 10 CCS nodes is larger than that with 8 nodes. Therefore, we determined that 8 CCS nodes are adequate.

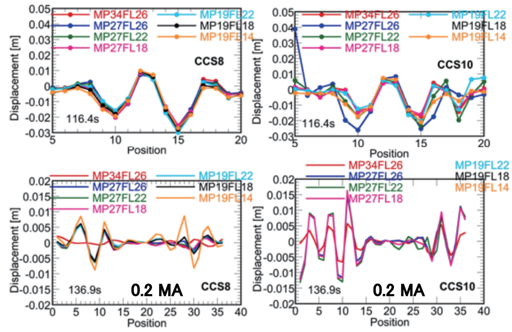

Fig. 9 Reconstruction error at the LCFS with weight of 10 and large CCS at 116.4 s and 136.9 s.

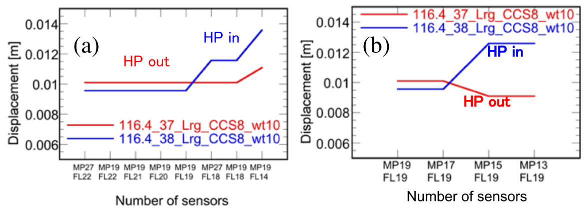

Fig. 10 Reconstruction error at the HP with reduction of (a) FLs and (b) magnetic probes (MPs) at 116.4 s.

4. Investigating the Minimum Number of Sensors

For a large device, the cost of an FL is much higher than that of an MP because of the installation cost. Therefore, we first reduced the number of FLs, as shown in Fig. 10 (a). The minimum required number of FLs was found to be 19 because 18 FLs cannot be allowed even if the number of magnetic sensors increases by 1.5 times compared to that in the case of 19 FLs. Next, we reduced the MPs with 19 FLs, as shown in Fig. 10 (b). Finally, the minimum number of FLs and MPs was decided to be 19 and 17, respectively, for an HP error within 1 cm. In comparison with the accuracy of the maximum number of sensors (MP34FL26), that of the LCFS with a minimum number of sensors (MP17FL19) is reasonable (Fig. 11). After the exploration of the same procedure in the case when sensors were not used on the SP, we determined the minimum number of magnetic sensors, as shown in Fig. 12.

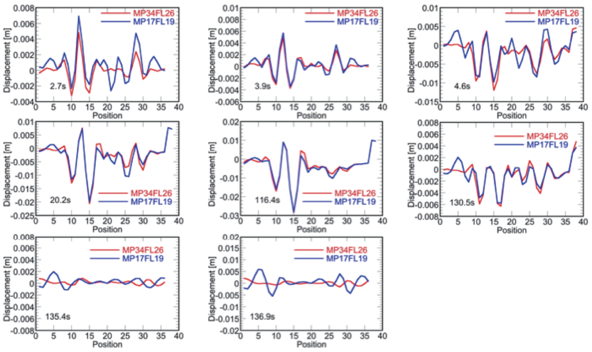

Fig. 11 Comparison of the LCFS errors with the maximum number of sensors (MP34FL26) and with the minimum number of sensors (MP17FL19).

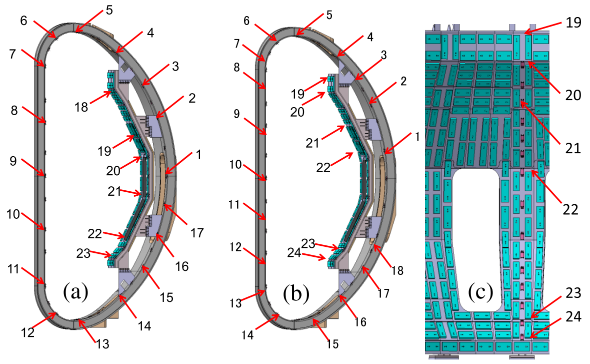

Fig. 12 A set of minimum number of (a) MPs, (b) FLs and (c) FL on the stabilizing plate (SP).

5. Conclusion

The minimum number of the MPs and FLs required for the accurate reconstruction of JT-60SA plasma shape was investigated using the CCS method. Before applying this method, the optimization of the CCS reconstruction parameters with the JT-60SA plasma was performed. We found that the HP errors reduced as the number of CCS nodes increased However, reconstruction failures increased as the number of CCS nodes increased because of a small number of sensors. A larger CCS also reduces the reconsruction error. To reduce the HP error, it is effective to weight the signals of FLs around HP for the least squares method. Finally, the HP error reduced to within 1 cm with a large CCS, a weight of 10 and 8 CCS nodes. The maximum external and internal errors at the LCFS were within 3 and 1cm, respectively. Recently, additional optimization were performed [8]. The minimum number of sensors required for JT-60SA was determined. The number of MPs was 17 for VV and 6 for the SP, i.e., 23 MPs in total. The number of FLs was18 for VV and 6 for SP, i.e., 24 FLs in total. Actually, only 19FLs will be used. However, we will install as many FLs as possible because the replacement of FLs is difficult after the completion of a tokamak.

[1] H. Shirai, P. Barabaschi and Y. Kamada, Fusion Eng. Des. **109-111**, Part B, 1701 (2016), Proceedings of the 12th International Symposium on Fusion Nuclear Technology-12 (ISFNT-12).
[2] M. Takechi, G. Matsunaga, S. Sakurai, T. Sasajima, J. Yagyu, R. Hoshi, Y. Kawamata, K. Kurihara, T. Nishikawa, T. Ryo, S. Kagamihara and K. Nakamura, Fusion Eng. Des. **96-97**, 985 (2015), Proceedings of the 28th Symposium On Fusion Technology (SOFT-28).
[3] K. Kurihara, Fusion Eng. Des. **51-52**, 1049 (2000).
[4] K. Kenichi, K. Youichi, S. Michiharu, H. Hiroki, Y. Izuru, S. Takahiro, O. Toshihiro, I. Shunsuke and JT-60 Team, Fusion Eng. Des. **74**, 527 (2005).
[5] Y. Miyata, S.H. Hahn, T. Suzuki, S. Ide, J. Chung, J.G. Bak and W.H. Ko, Phys. Plasmas **21**, 032502 (2014).
[6] M. Itagaki, A. Sanpei, S. Masamune and K. Watanabe, Plasma Fusion Res. **9**, 1402046 (2014).
[7] M. Itagaki, K. Ishimaru, Y. Matsumoto, K. Watanabe, R. Seke and Y. Suzuki, Plasma Fusion Res. **8**, 1402134 (2013).
[8] Y. Miyata, T. Suzuki, M. Takechi, H. Urano and S. Ide, Rev. Sci. Instrum. **86**, 073511 (2015).